J Therm Anal Calorim (2017) 127:1467–1477
DOI 10.1007/s10973-016-6005-6

Interactions of cyanidin and cyanidin 3-*O*-β-glucopyranoside with model lipid membranes

Violeta Rakić[1] · Ajda Ota[2] · Dušan Sokolović[3] · Nataša Poklar Ulrih[2]

Received: 18 July 2016 / Accepted: 25 November 2016 / Published online: 8 December 2016

Abstract Cyanidin and cyanidin 3-*O*-β-glucopyranoside (Cy3Glc) are flavonoids that have several biological properties, including as antioxidants. The interactions of cyanidin and Cy3Glc with model lipid membranes differing in surface charge and phase state were investigated using differential scanning calorimetry and fluorescence emission polarization spectrometry. Differential scanning calorimetry shows that cyanidin and Cy3Glc have no effects on the phase transition of zwitterionic liposomes composed of the 1,2-dipalmitoyl-*sn*-glycero-3-phosphocholine (DPPC) and negatively charged liposomes composed of 1,2-dipalmitoyl-*sn*-glycero-3-phosphoglycerol (DPPG) at pH 7.0. Emission polarization spectrometry using 1,6-diphenyl-1,3,5-hexatriene (DPH) and N,N,N-trimethyl-4-(6-phenyl-1,3,5-hexatrien-1-yl)phenylammonium p-toluenesulfonate (TMA-DPH) probes shows that cyanidin slightly increases the polarization of DPPC and DPPG liposomes in the gel state at 298.15 K. Significant ordering effects of cyanidin on DPPC liposomes in the liquid state at 318.15 K and no effect on the liquid state of DPPG at 318.15 K were observed using the DPH and TMA-DPH probes. Cy3Glc causes no change in polarization regardless the gel or liquid-disordered state of DPPC or DPPG liposomes. Cy3Glc due to its glucoside moiety is too bulky to partition into water–lipid interface or between the nonpolar acyl chains of membranes. The results of this work may contribute to understanding the low bioavailability of glycosides.

Keywords Cyanidin · Cyanidin 3-glucoside · DPPC and DPPG model membranes · DSC · Fluorescence emission polarization of DPH and TMA-DPH

Introduction

Anthocyanins are a group of flavonoids that are found in various fruits and vegetables and have several biological activities, including antioxidant activity, which plays a vital role in the prevention of neuronal and cardiovascular illnesses, cancer and diabetes, among others [1]. Epidemiological studies have suggested that anthocyanins have cardioprotective functions in human [2], and other studies have suggested that anthocyanins inhibit tumor-cell growth in vitro and suppress tumor growth in vivo [3].

The high antioxidant potential of anthocyanins has been shown in vitro using several antioxidant systems that are based on quenching free radicals in cell-free systems. These tests have included radical scavenging capacity, using 2,2′-diphenyl-1-picrylhydrazyl [4–6] or 2,2′-azino-bis-(3-ethylbenzothiazoline-6-sulfonic acid) [6], ferric-reducing antioxidant activity [7], oxygen radical absorbance activity [8–10], and antioxidant activity in human low-density lipoprotein [5, 11], methyl linoleate [5, 12], and liposome [11] systems.

In cell membranes, free radical peroxidation of lipids disrupts the structural and protective functions of the lipids, which can result in several pathological events [13]. The molecular mechanisms of polyphenol antioxidant action

✉ Nataša Poklar Ulrih
natasa.poklar@bf.uni-lj.si

[1] College of Agriculture and Food Technology, Ćirila i Metodija 1, Prokuplje 18400, Serbia

[2] Department of Food Science and Technology, Biotechnical Faculty, University of Ljubljana, Jamnikarjeva 101, 1000 Ljubljana, Slovenia

[3] Faculty of Medicine, University of Niš, Blvd. Dr Zorana Djindjica 81, Nis 18000, Serbia

are poorly understood, and it has been suggested that the antioxidant properties of polyphenols lies in their ability to insert into cell membranes and to modify the lipid packing order, and thus fluidity. Flavonoids and isoflavonoids can partition into the hydrophobic core of membranes and cause dramatic decreases in lipid fluidity in this region of the membrane [14, 15]. Localization of flavonoids and isoflavonoids in the membrane interiors and the resulting fluidity restrictions to the membrane components might sterically hinder diffusion of free radicals, and thereby decrease the kinetics of free radical reactions [14, 15].

Following their ingestion, anthocyanins have been detected intact in blood [16, 17], at considerably shorter times than those seen for other flavonoids [18]. They are also found in plasma as intact glycosylated compounds. The rapid diffusion of anthocyanins across the gastro-intestinal barrier is via membrane transporters that promote their specific, sequential translocation from the gastro-intestinal lumen into epithelial cells, and from these epithelial cells into the blood [19]. Bilitranslocase is a membrane transporter in the gastric epithelium that appears to be relatively specific for anthocyanins. The poor bioavailability of anthocyanins appears to arise as they are transported into intestinal cells by a carrier-mediated mechanism that has a high affinity, although low capacity, of transport. Contrary to many other organic anions, the anthocyanins are apparently not transported by intestinal membrane carriers other than bilitranslocase, although this needs to be further investigated [19]. With biological and model membranes, the interactions between some flavonoids and lipid bilayers result in either their binding at the lipid–water interface or their distribution into the hydrophobic core of the membrane, with these different locations being determined by the chemical properties of the flavonoids [20].

To better understand the antioxidant activities and transport of cyanidin and cyanidin 3-*O*-β-glucopyranoside (Cy3Glc) across membranes, it is thus important to determine their locations in the membranes and their effects on the lipid packing order, and hence the membrane fluidity. In the present study, we investigated the interactions of cyanidin and Cy3Glc with model lipid membranes that differ in surface charge and phase state (gel or liquid). The interaction of cyanidin and Cy3Glc with one of the main membrane lipids, namely 1,2-dipalmitoyl-*sn*-glycero-3-phosphocholine (DPPC), and its negatively charged counterpart 1,2-dipalmitoyl-*sn*-glycero-3-phospho-(1′-*rac*-glycerol) (DPPG) as model membranes was studied. DPPC is one of the main lipids in eukaryotic cell membranes [21], and the usage of DPPC in membrane studies is very common [22–26]. They are responsible for several features of the bilayer like stability and semipermeable properties [27]. DPPG is chosen as an experimental model lipid since it is the negatively charged counterpart of DPPC and so is used in order to understand the effect of charge status in cyanidin and Cy3Glc-model membrane interactions as reported in other studies [25, 28–31]. DPPG has the same acyl chain length with DPPC, but has negative charge and is used to understand the charge effect on bioactive molecules–membrane interactions [25, 26, 28–31]. It is known that a difference in the phospholipid head group causes different intermolecular interactions, drawing to different packing abilities [31, 32]. Providing such further understanding of the effects of cyanidin and Cy3Glc on these biophysical properties of membranes can help in the determination of the mechanism(s) of their action(s) as antioxidants and of their transport through cell membranes. Here, the effects of cyanidin and Cy3Glc on the gel-to-liquid crystalline phase transition (L_{β}'–P_{β}'–L_{α} phase transition divided into pre-transition, L_{β}'–P_{β}', and main transition, P_{β}'–L_{α}) of model membranes of the zwitterionic DPPC and of the negatively charged DPPG were investigated using differential scanning calorimetry (DSC). The localization of cyanidin and Cy3Glc in these DPPC and DPPG membranes and their effects on the membrane fluidity were studied using fluorescence emission polarization of the fluorophores 1,6-diphenyl-1,3,5-hexatriene (DPH) and N,N,N-trimethyl-4-(6-phenyl-1,3,5-hexatrien-1-yl)phenylammonium p-toluenesulfonate (TMA-DPH).

Materials and methods

Chemicals and reagents

The chloride salts of cyanidin and Cy3Glc were from Polyphenols Laboratories AS (Sandnes, Norway) (Fig. 1). The DPPC and DPPG (sodium salt) phospholipids were from Avanti Polar Lipids (Alabaster, AL, USA). The fluorophores DPH and TMA-DPH were from Aldrich Chemical Co. (Milwaukee, WI, USA). The 4-(2-hydroxyethyl)-1-piperazineethanesulfonic acid (HEPES) was from Sigma-Aldrich (Steinheim, Germany). All of the other chemicals used were of analytical grade and were from Merck (Darmstadt, Germany). The water used for all experiments was purified using a Milli-Q system from Millipore (resistivity >18 MΩ cm) (Bedford, MA, USA).

Preparation of vesicles

Multilamellar vesicles (MLVs) were prepared from DPPC and DPPG using the thin-layer-film method [36]. Briefly, DPPC and DPPG were dissolved separately in methanol/chloroform (DPPC: 3:7, v/v; DPPG: 1:9, v/v) and transferred to rotary flasks, where the solvents were completely

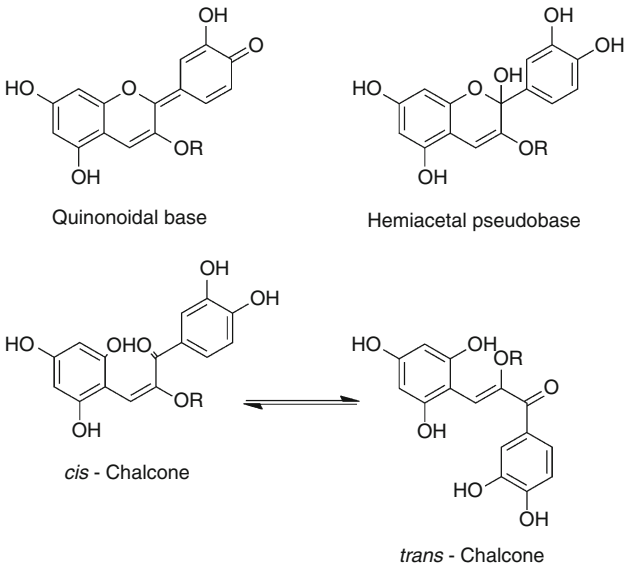

Fig. 1 Chemical structures of cyanidin and Cy3Glc in aqueous solutions at pH 7.0 [33–35]. At C-3 for cyanidin $R = H$, for Cy3Glc $R = Glc$

evaporated off under reduced pressure (1000 Pa), followed by vacuum drying. After these lipids had formed a thin film, HEPES (20 mmol dm^{-3}, pH 7.0) heated to 323.15 K (above the gel-to-liquid crystalline phase transition [T_m] for DPPC and DPPG) was added, and the mixture was vortexed vigorously to form MLVs. The final lipid concentration of the vesicles was 2.0 mg cm^{-3}.

For DSC measurements, the DPPC and DPPG MLVs were used at a final concentration of 0.5 mg cm^{-3}, in the same buffer. For fluorescence measurements, small unilamellar vesicles (SUVs) were prepared from these MLVs by disintegration with a high-intensity ultrasonic cell disrupter Vibracell VCX 750 (Sonics and Materials, Newtown, CA, USA) in an ice-cold bath for a total of 15 min, as continuously repeated 10 s on–off cycles at 40% amplitude of 750 W [37]. The SUVs for the fluorescence measurements were prepared in 20 mmol dm^{-3} HEPES, pH 7.0, at the final DPPC and DPPG concentrations of 0.1 mg cm^{-3}.

Differential scanning calorimetry

To follow the effects of cyanidin and Cy3Glc on the gel-to-liquid phase transitions of MLVs composed of DPPC or DPPG (0.5 mg cm^{-3}), a NANO DSC series III system was used (Calorimetry Science, Provo, UT, USA). The phase transitions of the MLVs at pH 7.0 (20 mmol dm^{-3} HEPES buffer) were monitored with cyanidin and Cy3Glc at a 1:1 and 2:1 molar ratio to DPPC, and a 1:1 molar ratio to DPPG. The molar ratio, $R = 2:1$, of cyanidin and Cy3Glc to DPPC was used to intensify the magnitude of interactions. To prepare cyanidin/Cy3Glc-containing liposomes, the required amount of cyanidin/Cy3Glc from stock solution was initially put into the sample tube, excess of methanol was evaporated by nitrogen flux, and then liposomes suspension (0.5 mg cm^{-3}) in HEPES buffer was added and vortexed. The samples were degassed under vacuum and loaded into the calorimetric cell, in which they were heated/cooled repeatedly in the temperature range of 283.15–343.15 K, with a heating/cooling rate of 1 K min^{-1}. The first DSC scan was used to determine the temperature of pre-transition (T_{pre}), the temperature of gel-to-liquid lipid-phase transition (T_m), and the model-independent calorimetric enthalpy (ΔH_{cal}). The subsequent scans were used to determine the reversibility of the lipid-phase transition. The OriginPro 8.1 software (OriginLab Corporation, Northampton, MA, USA) was used to evaluate the enthalpies and temperatures of transition from the DSC curves.

Florescence polarization

The fluorescence polarization measurements of DPH and TMA-DPH were performed in a 10-mm-path-length cuvette using a Cary Eclipse fluorescence spectrophotometer (Varian, Mulgrave, Victoria, Australia) equipped with a magnetic stirrer, a thermostatically controlled cell holder, and a digital thermocouple that allowed direct temperature measurements of the samples. The temperatures of 298.15 and 318.15 K were used for the DPPC and DPPG SUVs (above and below the DPPC/DPPG main transitions). Varian auto-polarizers were used, with slit widths with a normal band-pass of 5 nm for both excitation and emission. DPH and TMA-DPH were added to 0.1 mg cm^{-3} solutions of SUVs of pure DPPC or DPPG in 20 mmol dm^{-3} HEPES, pH 7.0. The final concentrations of DPH and TMA-DPH were 0.5 μmol dm^{-3} and 8 μmol dm^{-3}, respectively. Solutions of these DPPC or DPPG SUVs with DPH or TMA-DPH were titrated using the addition of aliquots of 2 mmol dm^{-3} cyanidin or Cy3Glc solutions in methanol, to obtain cyanidin/Cy3Glc:DPPC/DPPG molar ratios from 1:1 to 2:1. The control experiment was performed to follow the effect of methanol on DPPC or DPPG SUVs with DPH or TMA-DPH. After each cyanidin and Cy3Glc addition, the samples were allowed to equilibrate for 10 min. DPH and TMA-DPH fluorescence emission polarization was measured in the presence of these DPPC or DPPG SUVs as a function of the concentrations of cyanidin and Cy3Glc. An excitation wavelength of 358 nm was used, with the excitation polarizer oriented in a vertical position, while the vertical and horizontal components of the polarized emission light were recorded through a monochromator at 410 nm, for both of the probes. The values of the G-factor (the ratio of the sensitivities of the

detection system for the vertically and horizontally polarized light) were determined separately for each sample. The DPH and TMA-DPH polarization (P) was calculated using the built-in software of the instrument, according to Eq. (1):

$$P = \frac{I_{||} - \mathrm{GI}_{\perp}}{I_{||} + \mathrm{GI}_{\perp}} \quad (1)$$

where $I_{||}$ and $I_{\perp}$ are the fluorescence intensities of the vertically and horizontally polarized emissions, respectively, when the samples were excited with vertically polarized light [38].

Kinetic stability of cyanidin and cyanidin 3-*O*-β-glucopyranoside at 328.15 K

To get insight the kinetic stabilities of cyanidin and Cy3Glc at temperature above the DPPC/DPPG main phase transition (328.15 K) in 20 mmol dm^{-3} HEPES, pH 7.0, the absorption spectra of the cyanidin and Cy3Glc solutions were recorded in 30 min time intervals. The chloride salts of cyanidin and Cy3Glc were dissolved in 20 mmol dm^{-3} HEPES, pH 7.0, to the final concentration of 0.25 mmol dm^{-3}. The absorption spectra (190–900 nm) of these cyanidin and Cy3Glc solutions were recorded at 328.15 K using a Cary 100 Bio UV–Vis spectrophotometer (Varian, Mulgrave, Victoria, Australia) in a thermostated 10-mm-path-length quartz cell, using a digital thermocouple that allowed direct temperature measurements of the samples, and with 20 mmol dm^{-3} HEPES, pH 7.0, as the reference. Each spectrum was corrected for the blank solution. The decreases in absorbance, as percentages relative to the initial absorbance at time zero (t_0), are plotted as a function of time at 568 nm for cyanidin and at 559 nm for Cy3Glc. The data were fitted by built-in mathematical model (ExpDec1 and ExpDec2) for first-order reaction from which the rate constant of reaction k_1 and k_2 were obtained using the OriginPro 8.1 software (OriginLab Corporation, Northampton, MA, USA).

Results and discussion

Energetic impact of cyanidin and cyanidin 3-*O*-β-glucopyranoside on DPPC and DPPG gel-to-liquid phase transition

Lipid-phase transitions can be followed using DSC, which measures heat flow as a function of temperature [26]. The main gel-to-liquid phase transition of lipids occurs at the transition temperature, T_m, generally gives rise to a very intense and sharp peak in the heat capacity and corresponds to P_β'–L_α transition from ripple gel intermediate phase (P_β') to liquid crystalline (L_α). On the other hand, the pretransition temperature, T_{pre}, is usually detected as a much less intense and broader peak at lower temperatures and corresponds to L_β'–P_β' transition from quasi-lamellar (L_β') to ripple gel intermediate phase (P_β') [26]. To study the cyanidin and Cy3Glc lipid interactions, DPPC and DPPG MLVs were chosen as the model membranes. Phosphocholine and phosphoglycerol lipids with the same acyl chains are known to show similar thermal behaviors [39].

Figures 2 and 3 show the lipid thermotropic phase behaviors of the DPPC and DPPG MLVs, respectively, without and with the addition of cyanidin and Cy3Glc. The T_m of DPPC and DPPG in the absence of cyanidin and Cy3Glc was 314.35 (±0.2) K and 313.55 (±0.2) K, respectively (Table 1). These data are in agreement with the literature data [26, 40, 41]. The main transition is ascribed to the reorientation of acyl chains from an ordered structure into a tilted configuration, as the well-known L_β'–L_α phase transition. This thermotropic behavior can be studied using DSC, and it can be influenced by small molecules that can dissolve in the ordered lipid bilayer structure [42, 43].

In Fig. 2, the effects of cyanidin and Cy3Glc addition on the thermotropic phase behavior of the DPPC MLVs can be seen at the 2:1 molar ratio of cyanidin or Cy3Glc to DPPC. At the molar ratio of 1:1, there were no effects of cyanidin and Cy3Glc on the phase transition of these DPPC MLVs. Even at the 2:1 molar ratio, there were also no effects of cyanidin and Cy3Glc on the phase transition of DPPC in this temperature range from 283.15 to 343.15 K (Fig. 2). The integral of the excess heat capacity gives the enthalpy change, ΔH_{cal}, that is associated with gel-to-liquid transition. The thermodynamic parameters of this transition are given in Table 1. Detailed inspection of Table 1 reveals that cyanidin and Cy3Glc have no significant effects on the

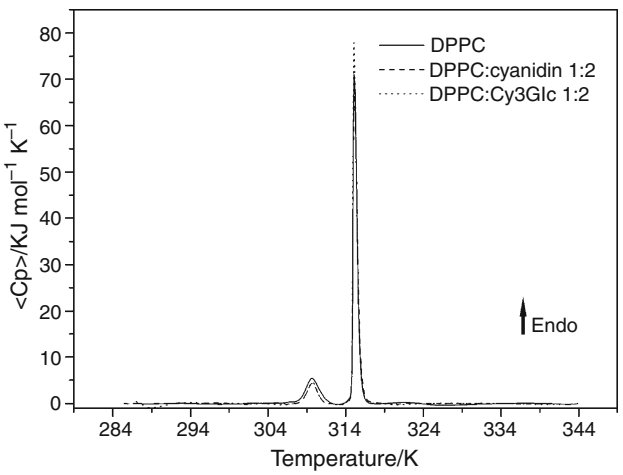

Fig. 2 Differential scanning calorimetry profiles in the absence and presence of cyanidin and Cy3Glc for the DPPC MLVs at a 2:1 molar ratio ($n_{cy/Cy3Glc}/n_{DPPC}$), respectively

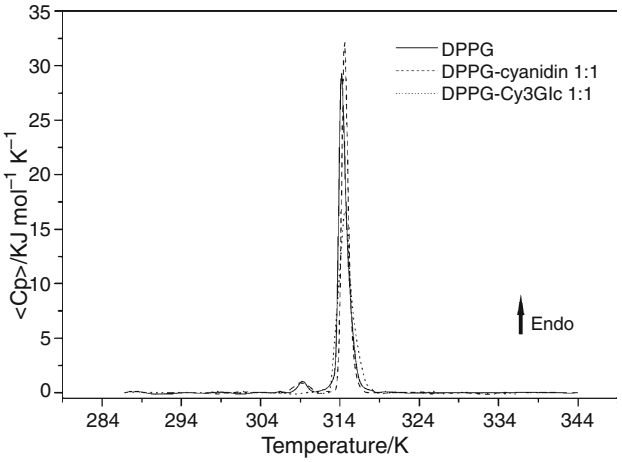

Fig. 3 Differential scanning calorimetry profiles in the absence and presence of cyanidin and Cy3Glc for the DPPG MLVs, at a 1:1 molar ratio ($n_{cy/Cy3Glc}/n_{DPPG}$), respectively

thermal and enthalpic stabilization of the DPPC MLVs at 2:1 ratio of cyanidin/Cy3Glc to DPPC MLVs, as the temperature and enthalpy of the gel-to-liquid transition do not change significantly (Table 1). Based on this DSC profile, it is likely that there are no significant interactions between the neutral cyanidin and Cy3Glc with these zwitterionic DPPC MLVs.

In Fig. 3, the effects of cyanidin and Cy3Glc on the thermotropic phase behavior of the DPPG MLVs are shown, at a molar ratio of 1:1 for cyanidin/Cy3Glc to DPPG.

The interactions of cyanidin and Cy3Glc with the negatively charged DPPG MLVs slightly change T_m (Fig. 3; Table 1). The T_{pre} in the presence of cyanidin does not change, while the pre-transition peak in the presence of Cy3Glc disappears. The main transition peak in the thermograms became smaller and broader, although the enthalpy did not change (Fig. 3; Table 1). Cyanidin and Cy3Glc have no effects on enthalpic stabilization/destabilization of the main transition of these DPPG MLVs at molar ratio 1:1 (Table 1).

Thus from the DSC data, cyanidin and Cy3Glc thermally and enthalpically do not stabilize the negatively charged DPPG MLVs (Fig. 3; Table 1). The polar headgroup of DPPG is negative, and it has two -OH groups on the glycerol moiety. At pH 7.0, cyanidin and Cy3Glc are in the neutral form of quinonoidal bases, hemiacetal pseudobases and chalcone [33, 44] (Fig. 1) which cannot interact electrostatically as we would have expected. The negligible changes in the enthalpy of the main transition, ΔH_{cal}, that are generally seen for cyanidin and Cy3Glc might be due to a superficial interaction of cyanidin and Cy3Glc with lipids at the level of the polar head groups of DPPC and DPPG as it was observed before for some flavonoides [45].

Effects of cyanidin and cyanidin 3-*O*-β-glucopyranoside on DPH and TMA-DPH polarization in model lipid membranes of DPPC and DPPG

Steady-state polarization measurements were made for the DPPC and DPPG SUVs at different temperatures (so at different phase states of the lipids) and in the presence of cyanidin and Cy3Glc, at different molar ratios. Fluorescence polarization was measured using two fluorescent probes: DPH and TMA-DPH. These two fluorescence probes were used because each of them embeds itself in different regions of the lipid bilayer. The DPH probe is an apolar molecule which is incorporated into the hydrophobic region of the liposome bilayer with its long axis parallel to the acyl chains [41, 46], while the TMA-DPH probe is positioned at the fourth carbon atom in the transient region between the hydrophobic and hydrophilic parts of the bilayer [41]. This differential incorporation of these probes provides insight into the structural changes caused by the

Table 1 Thermodynamic profiles of DPPC and DPPG MLVs (pH 7.0) in the absence and presence of cyanidin and Cy3Glc at different molar ratios (*R*)

MLV[a] conditions	*R*	T_m/K	ΔH_{cal}/kJ mol^{-1}	$\Delta T_{1/2}$/K
DPPC	–	314.35 ± 0.2	44.0 ± 2.0	0.6 ± 0.1
Cyanidin + DPPC[b]	2:1	314.35 ± 0.2	44.8 ± 2.0	0.6 ± 0.1
Cy3Glc + DPPC[b]	2:1	314.35 ± 0.2	46.3 ± 2.0	0.6 ± 0.1
DPPG	–	313.55 ± 0.2	36.0 ± 2.0	1.1 ± 0.1
Cyanidin + DPPG	1:1	313.75 ± 0.2	35.3 ± 2.0	0.9 ± 0.1
Cy3Glc + DPPG	1:1	313.75 ± 0.2	35.6 ± 2.0	1.8 ± 0.1

[a] MLVs at 0.5 mg cm^{-3} DPPC/DPPG

[b] The higher molar ratio, $R = 2{:}1$ of cyanidin and Cy3Glc to DPPC, was used to intensify the magnitude of interactions

Data are mean ± SD ($n = 3$)

incorporation of cyanidin and Cy3Glc [14, 41, 46, 47]. The degrees of DPH and TMA-DPH fluorescence polarization reflect the degree to which the molecules of these fluorescence probes are reoriented during the excited state. This is seen as a decrease in the degree of reorientation (and thus an increase in that of polarization) in an environment in which motion is restricted, i.e., a closely (tightly) packed, ordered (less fluid) lipid environment. There is the greatest polarization (i.e., the lowest fluidity) with the highest gel state of the lipids and the lowest in the liquid-disordered state and intermediate in the liquid-ordered state [48].

These data from the steady-state DPH and TMA-DPH polarization measurements for the addition of cyanidin or Cy3Glc to the DPPC SUVs at 298.15 K and 318.15 K are shown in Fig. 4.

To study the effects of cyanidin and Cy3Glc on the DPPC SUV properties in a gel-crystalline state, steady-state DPH and TMA-DPH polarization measurements were performed at 298.15 K. The polarization of DPH before the addition of cyanidin or Cy3Glc to these DPPC SUVs was 0.396. The addition of cyanidin to DPPC increased the polarization of DPH in the whole concentration range up to molar ratios 2.0 (Fig. 4a). These data indicate that cyanidin has a slight membrane-ordering effect on DPPC SUVs in the gel state. In comparison, Cy3Glc has lower effect on the lipid hydrophobic region, where the non-specific DPH probe is located (Fig. 4b).

The polarization of TMA-DPH in these DPPC SUVs at 298.15 K and before the addition of cyanidin or Cy3Glc was 0.430, and this increased only slightly after the addition of cyanidin or Cy3Glc (Fig. 4c, d). As indicated by the fluorescence polarization at the interphase between the hydrophilic and hydrophobic parts of these DPPC SUV membranes (i.e., the level at which the TMA-DPH probe is incorporated), cyanidin caused a small and constant increase in polarization (ordering) of DPPC SUVs (Fig. 4c).

To study the effects of cyanidin and Cy3Glc on the DPPC and DPPG SUV properties in a liquid state, we performed steady-state DPH polarization measurements at 318.15 K (Fig. 4a, b). The transition temperature of DPPC is 314.15 K, and so at 318.15 K the DPPC in these SUVs is in the liquid unordered state. Before addition of cyanidin or Cy3Glc, the polarization of DPH in the DPPC SUVs at 318.15 K was 0.147. With increased cyanidin addition, the DPH polarization in the DPPC SUVs increased, indicating

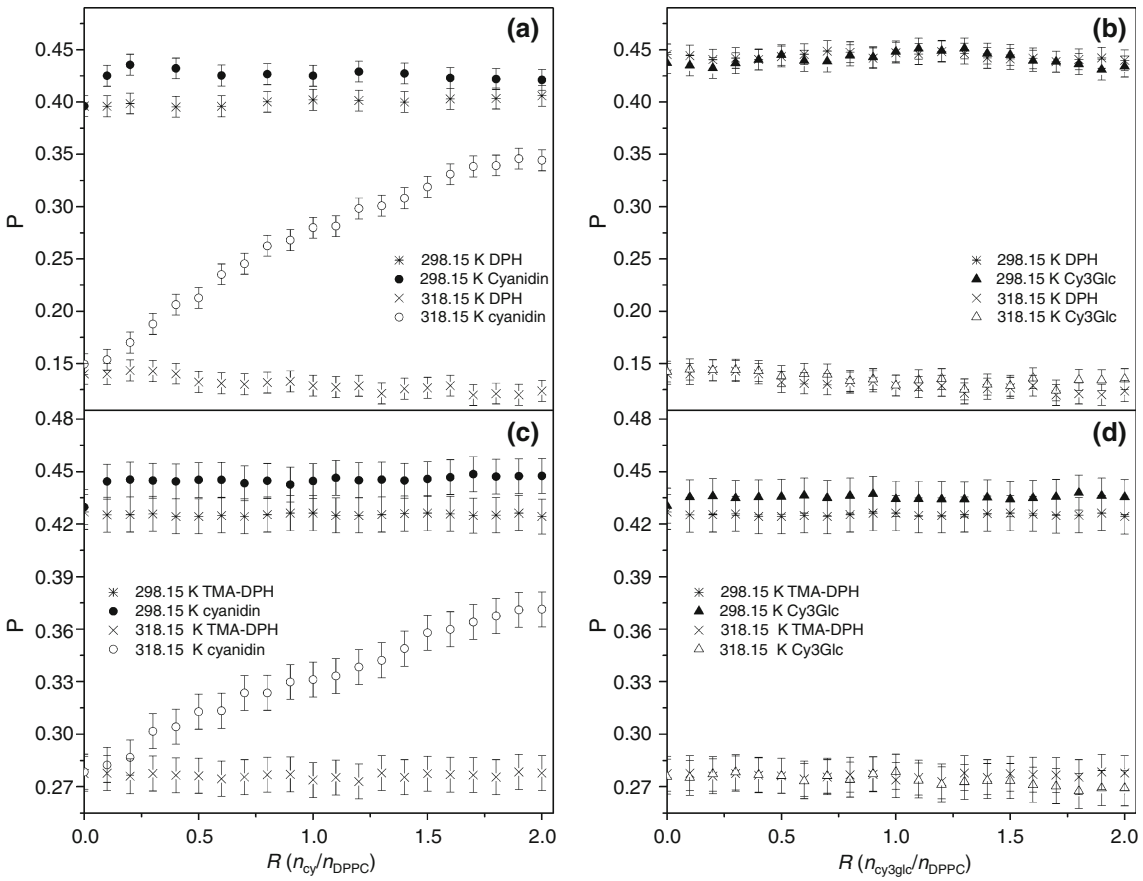

Fig. 4 Polarization (*P*) of the fluorophors DPH (**a**, **b**, *crosses*) and TMA-DPH (**c**, **d**, *crosses*) with the addition of cyanidin (**a**, **c**, *circles*) and Cy3Glc (**b**, **d**, *triangles*) to the DPPC SUVs at different molar ratios (*R*) at 298.15 K (*closed symbols*) and 318.15 K (*open symbols*)

that cyanidin had a strong membrane-ordering effect on the liquid-state DPPC SUVs (Fig. 4a), while Cy3Glc had no effects (Fig. 4b).

Before the addition of cyanidin or Cy3Glc, the polarization of TMA-DPH in these DPPC SUVs in the liquid state at 318.15 K was 0.277, and after the addition of cyanidin, the polarization increased across the whole concentration range (Fig. 4c). However, with the addition of Cy3Glc, there were no effects on the polarization of TMA-DPH in these DPPC SUVs at 318.15 K (Fig. 4d).

A comparison of cyanidin and Cy3Glc can explain this effect, considering that cyanidin has a polar surface area of 114.29 $Å^2$ and a partition coefficient between octanol and water (log P_3) of 3.05, and Cy3Glc has a polar surface area of 193.44 $Å^2$ and a log P_3 of 0.39 [49]. Thus, cyanidin is a less polar and smaller molecule compared to Cy3Glc, and these data indicate that at the temperature of 318.15 K, where the DPPC SUV membranes are in a liquid state, cyanidin affects the polarization values of DPH and TMA-DPH in DPPC SUVs. It is likely that cyanidin can partly insert into the water–lipid interface of SUV and enhance the order of nonpolar acyl chains of DPPC. The discrepancy observed by studying the cyanidin interactions with DPPC lipids by polarization measurements and DSC can be due to different form of liposomes, SUV and MLV, respectively. Several studies showed that the curvature of the membrane due to the macromolecular size and shape affects the thermodynamic properties. DSC scans showed that small unilamellar vesicles (SUVs) have lower enthalpic peaks and greater widths compared to multilamellar vesicles (MLVs). SUVs also have more mobility and less order in the hydrocarbon chains [50].

It can thus be postulated that cyanidin becomes concentrated in the hydrophobic part of these DPPC SUVs and in the transient region between the hydrophobic and hydrophilic parts of the membrane. According to Arora et al. [14], a greater degree of structural order and rigidity of membranes can reduce the mobility of free radicals in the lipid bilayer. Consequently, this decreased membrane fluidity would result in inhibition of lipid peroxidation due to the slow-down of free radical reactions [14]. It is interesting that these interactions do not have any impact on the thermal stability of these DPPC SUVs, as can be seen from the DSC data at molar ratio of 2 mol cyanidin to 1 mol lipid.

In addition to these neutral DPPC liposomes, we examined the effects of cyanidin and Cy3Glc on liposomes of the anionic lipid DPPG. The DSC study above (Fig. 3) showed, similarly as it was observed for DPPC liposomes, that cyanidin and Cy3Glc do not have significant effect on the thermodynamic parameters of gel-to-liquid transition (Table 1) of the DPPG MLVs. Therefore, the polarization measurements of DPH and TMA-DPH in the presence of these DPPG SUVs were performed at 298.15 K for the model membranes in the gel state, and at 318.15 K for the model membranes in a liquid-disordered state.

Thus, to study the effects of cyanidin and Cy3Glc on the DPPG membrane properties in the gel state, we perform steady-state DPH polarization measurements at 298.15 K with SUVs composed of DPPG (Fig. 5a, b). The polarization of DPH in these DPPG SUVs before the addition of cyanidin or Cy3Glc was 0.420. The addition of cyanidin caused an initial increase in polarization up to 0.437, while the addition of Cy3Glc caused no change in the polarization of DPH in DPPG lipids (Fig. 5a, b).These data indicate that cyanidin increases the ordering and decreases the dynamics of the phospholipid alkyl chains in the DPH environment; or in other words, the membranes initially become more ordered when they incorporate of cyanidin.

The polarization of TMA-DPH in this DPPG SUVs at 298.15 K before the addition cyanidin or Cy3Glc was 0.379. Cyanidin caused increase in the polarization of TMA-DPH, while Cy3Glc had no significant effect on the polarization in the whole concentration range (Fig. 5c, d). As the TMA-DPH probe is located in the interphase between the hydrophilic and hydrophobic parts of membrane, this indicates that this part of the lipid bilayer in gel state is affected by cyanidin but not with Cy3Glc.

As indicated above, the impact of cyanidin and Cy3Glc on the properties of these DPPG SUVs in the liquid state was studied at the temperature of 318.15 K, where the DPH polarization before the addition of cyanidin and Cy3Glc was 0.154. These DPPG SUVs were in a liquid-disordered state, and the addition of cyanidin or Cy3Glc had no significant effects on the DPH polarization (Fig. 5a, b). These data indicated that cyanidin and Cy3Glc have no effects on the DPPG SUV membrane properties at this temperature. Similar results were obtained when the TMA-DPH probe was used. The polarization of TMA-DPH in these DPPG SUVs at 318.15 K before addition cyanidin or Cy3Glc was 0.270, and this did not change after their addition (Fig. 5c, d).

Thus, at 298.15 K, cyanidin influences the structure of the DPPG liposomes in the gel state, while Cy3Glc does not. No effect of Cy3Glc on polarization was seen across the whole concentration range using the DPH or TMA-DPH membrane probe. It is likely that cyanidin and especially Cy3Glc do not interact with negatively charged groups of DPPG. They can interact on the surface of these liposomes (which will initially increase the surface rigidity) and then partially insert between the water–lipid interface, thus causing an increase in the rigidity of the acyl chains deeper in the liposome bilayer. This conclusion explains the data obtained with the DSC measurements, which show that cyanidin and Cy3Glc do not affect the

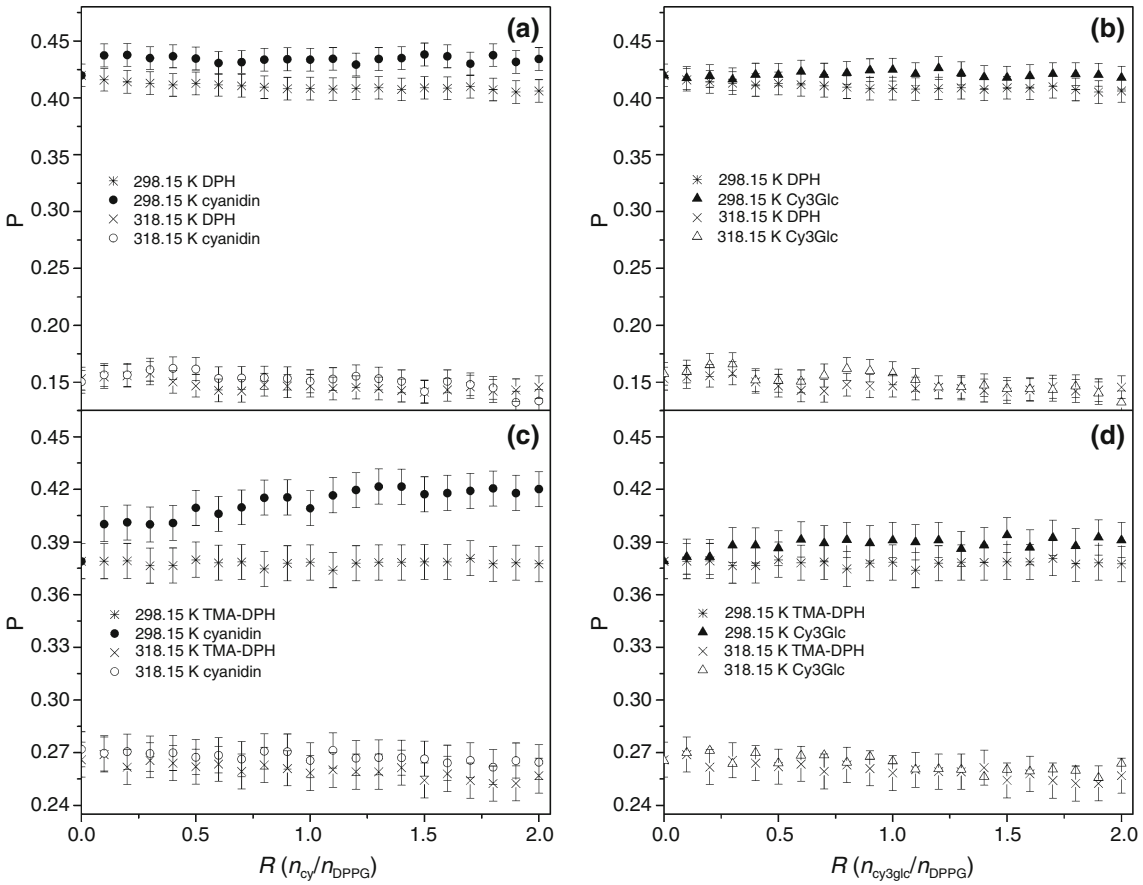

Fig. 5 Polarization (*P*) of the fluorophors DPH (**a**, **b**, *crosses*) and TMA-DPH (**c**, **d**, *crosses*) in the presence of DPPG SUVs at different molar ratios (*R*) of cyanidin (**a**, **c**, *circles*) and Cy3Glc (**b**, **d**, *triangles*) to DPPG at 298.15 K (*closed symbols*) and 318.15 K (*open symbols*)

thermal stability of DPPG liposomes (no observed increases in T_m).

Our data suggest that cyanidin influences the hydrophobic part and transient region between hydrophobic and hydrophilic parts of the DPPC liposomes in the liquid state by modifying the lipid packing order. Cyanidin thus increases the ordering and decreases the dynamics of the phospholipid alkyl chains of these liposomes in the liquid-disordered form. This appears to be because when the liposome membranes are in the liquid state, the less polar and smaller molecule of cyanidin (compared to Cy3Glc) can more easily insert between the nonpolar acyl chains of DPPC, and thus interact with them more easily. The more polar and bulkier Cy3Glc molecule (compared to cyanidin) has very little effect on the structure and energy of these neutral DPPC liposomes, irrespective of whether they are in the gel or liquid forms. Similar data were reported by Bonarska-Kujawa for selected anthocyanins interactions with erythrocytes and liposome membranes [47]. They conclude that the anthocyanins cause insignificant changes in the membrane structure and that their action is limited to the membrane surface, which indicates that the substances are effective and safe antioxidants [47].

Kinetic stability of cyaniding and cyanidin 3-*O*-β-glucopyranoside at 328.15 K

To eliminate any influences of thermal stability of cyanidin and Cy3Glc on the data for the fluorescence polarization measurements, we studied the kinetic stability of cyanidin and Cy3Glc at 328.15 K. The time-stability of cyanidin and Cy3Glc at 328.15 K was investigated using UV–Vis spectrometry, in 20 mmol dm^{-3} HEPES, pH 7.0, which was as used for the liposome preparation. The decrease in the absorbance at a constant wavelength as a function of time was expressed as the remaining absorbance relative to the starting absorbance at time zero (as percentages). These data obtained for cyanidin and Cy3Glc at 328.15 ± 0.1 K are presented in Figs. 6, 7.

For the given conditions here, the changes in absorbance with time for cyanidin differed from those for Cy3Glc. At t_0, cyanidin showed two main bands in the visible range, as one broad band with maximum absorbance at 568 nm with a smaller shoulder at around 515 nm, and a narrower band with maximum absorbance at 418 nm. Further, cyanidin showed one band in UV range, with a maximum at around 285 nm (Fig. 6a). These bands all showed decreases in

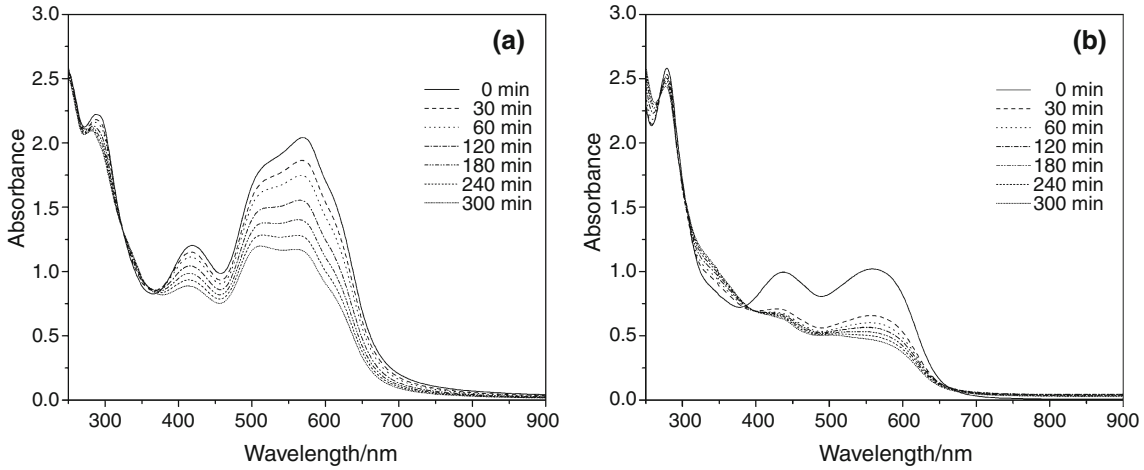

Fig. 6 Changes in the UV–Vis spectra of 0.25 mmol dm^{-3} cyanidin (**a**) and Cy3Glc (**b**) solutions during storage (up to 300 min) in 20 mmol dm^{-3} HEPES. pH 7.0, at 328.15 ± 0.1 K

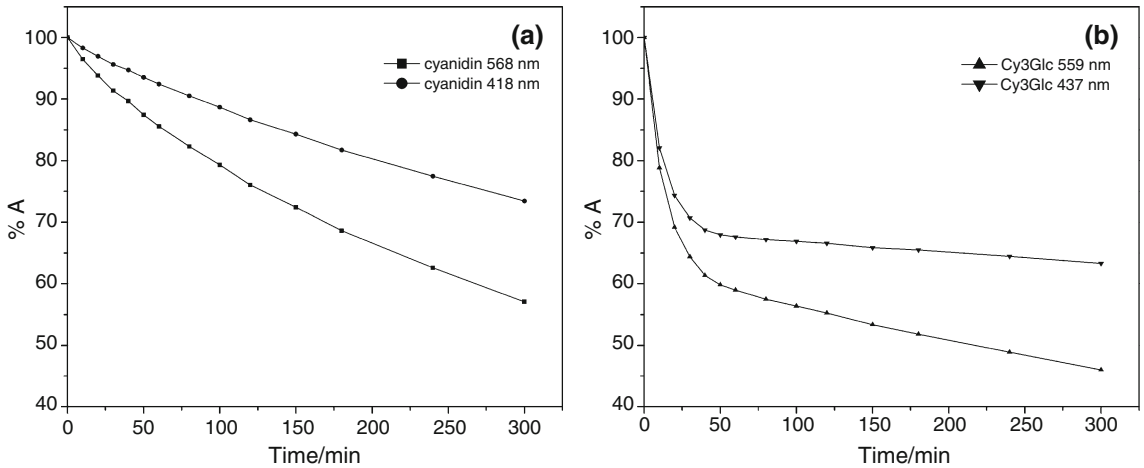

Fig. 7 Time-stability of cyanidin at 568 nm (*closed circle*) and Cy3Glc at 559 nm (*closed triangle*) during storage (up to 300 min) in 20 mmol dm^{-3} HEPES, pH 7.0, at 328.15 ± 0.1 K

absorbance with time, whereby the broad band (568 nm) showed greater decrease in absorbance compared to the narrower band (418 nm) (Fig. 6a). At t_0, Cy3Glc also showed two main bands in the visible range, with maximum absorbance at 559 and 437 nm, plus one band in the UV range, with a maximum at around 280 nm (Fig. 6b). In parallel with cyanidin, the Cy3Glc 559-nm band showed a greater decrease in absorbance compared to the Cy3Glc 437-nm band (Fig. 6b). Also, Cy3Glc showed a greater decrease in absorbance with time at 328.15 K than for cyanidin: after 10 min, 78.8% of Cy3Glc and 96.5% of cyanidin were intact, while after 30 min, 64.4% of Cy3Glc and 91.4% of cyanidin were intact. The rate constants of degradation obtained by fitting the curve for cyanidin was $(4.2 \pm 0.2) \times 10^{-3}$ min^{-1} and for Cy3Glc is $(7.76 \pm 0.07) \times 10^{-2}$ min^{-1} and $(1.2 \pm 0.9) \times 10^{-3}$ min^{-1}, respectively. The Cy3Glc is less kinetically stable at 328.15 K in comparison to cyanidin and degradation results in the formation of gallic acid, protocatechuic acid, and 2,4,6-trihydroxybenzaldehyde [51]. Since all of these degradation products are negatively charged, it is unlikely that they will interact with negatively charged lipids.

Conclusions

Previously, we have studied interactions of several phenolic compounds with model lipid membranes of different composition using a combination of fluorescence polarization, electron paramagnetic resonance spectroscopy (EPR) and differential scanning calorimetry (DSC). Our investigations with different flavonoids [tea catechins and synthetic antioxidant butylated hydroxytoluene (BHT)] indicated that total polar surface area

(TPSA) and polarity of flavonoids are the two main characteristics which influence the most the properties of model lipid membranes and that the studied flavonoids were bounded to the membrane surface predominantly via hydrogen bonds [52, 53]. It was also shown that composition of liposomes, especially cholesterol, significantly influences the interaction of flavonoids with cell membrane [52–54]. Here we have shown for the first time that the surface charge on the membrane and on the cyanidin and Cy3Glc does not play important role in binding at pH 7.0 because both compounds are at pH 7.0 in the form of quinonoidal bases and hemiacetal pseudobases and chalcone; therefore, further studies about the role of membrane charge additionally to the composition and the structure of flavonoids in their interactions with membranes are of great importance.

Acknowledgements The study was financially supported by Slovenian Research Agency through the research program P4-0121 (N.P.U.) and the bilaterally project between Republic of Slovenia and Republic of Serbia BI-RS/12-13-015 (N.P.U. and D.S). V.R. was partly financed by the CEPUS SI-8402/2010—bilateral scholarship.

References

1. Castañeda-Ovando A, de Pacheco-Hernández LM, Páez-Hernández ME, Rodríguez JA, Galán-Vidal CA. Chemical studies of anthocyanins: a review. Food Chem. 2009;113:859–71.
2. Chong MFF, Macdonald R, Lovegrove JA. Fruit polyphenols and CVD risk: a review of human intervention studies. Brit J Nutr. 2010;104:S28–39.
3. Chen P-N, Chu S-C, Chiou H-L, Chiang C-L, Yang S-F, Hsieh Y-S. Cyanidin 3-glucoside and peonidin 3-glucoside inhibit tumor cell growth and induce apoptosis in vitro and suppress tumor growth in vivo. Nutr Cancer. 2005;53:232–43.
4. Fukumoto LR, Mazza G. Assessing antioxidant and prooxidant activities of phenolic compounds. J Agr Food Chem. 2000;48:3597–604.
5. Kähkönen MP, Heinonen M. Antioxidant activity of anthocyanins and their aglycons. J Agr Food Chem. 2003;51:628–33.
6. Nayak B, Berrios JDJ, Powers JR, Tang J. Thermal degradation of anthocyanins from purple potato (cv. Purple Majesty) and impact on antioxidant capacity. J Agr Food Chem. 2011;59:11040–9.
7. Xiong S, Melton LD, Easteal AJ, Siew D. Stability and antioxidant activity of black currant anthocyanins in solution and encapsulated in glucan gel. J Agr Food Chem. 2006;54:6201–8.
8. Mazza G, Kay CD, Cottrell T, Holub BJ. Absorption of anthocyanins from blueberries and serum antioxidant status in human subjects. J Agr Food Chem. 2002;50:7731–7.
9. Stintzing FC, Stintzing AS, Carle R, Frei B, Wrolstad RE. Color and antioxidant properties of cyanidin-based anthocyanin pigments. J Agr Food Chem. 2002;50:6172–81.
10. Wang H, Cao G, Prior RL. Oxygen radical absorbing capacity of anthocyanins. J Agr Food Chem. 1997;45:304–9.
11. Satué-Gracia MT, Heinonen M, Frankel EN. Anthocyanins as antioxidants on human low-density lipoprotein and lecithin–liposome systems. J Agr Food Chem. 1997;45:3362–7.
12. Kähkönen MP, Hopia AI, Heinonen M. Berry phenolics and their antioxidant activity. J Agr Food Chem. 2001;49:4076–82.
13. Abuja PM, Albertini R. Methods for monitoring oxidative stress, lipid peroxidation and oxidation resistance of lipoproteins. Clin Chim Acta. 2001;306:1–17.
14. Arora A, Byrem TM, Nair MG, Strasburg GM. Modulation of liposomal membrane fluidity by flavonoids and isoflavonoids. Arch Biochem Biophys. 2000;373:102–9.
15. Arora A, Nair MG, Strasburg GM. Structure–activity relationships for antioxidant activities of a series of flavonoids in a liposomal system. Free Radical Bio Med. 1998;24:1355–63.
16. McGhie TK, Walton MC. The bioavailability and absorption of anthocyanins: towards a better understanding. Mol Nutr Food Res. 2007;51:702–13.
17. Prior RL, Wu X. Anthocyanins: structural characteristics that result in unique metabolic patterns and biological activities. Free Radical Res. 2006;40:1014–28.
18. Manach C, Williamson G, Morand C, Scalbert A, Rémésy C. Bioavailability and bioefficacy of polyphenols in humans. I. Review of 97 bioavailability studies. Am J Clin Nutr. 2005;81:230S–42S.
19. Keller RB, editor. Flavonoids: biosynthesis, biological effects and dietary sources. New York: Nova Science Publishers, Inc.; 2009.
20. Oteiza PI, Erlejman AG, Verstraeten SV, Keen CL, Fraga CG. Flavonoid-membrane Interactions: a protective role of flavonoids at the membrane surface? Clin Dev Immunol. 2005;12:19–25.
21. Deleu M, Crowet J-M, Nasir MN, Lins L. Complementary biophysical tools to investigate lipid specificity in the interaction between bioactive molecules and the plasma membrane: a review. Biochim Biophys Acta. 2014;1838:3171–90.
22. Severcan F, Sahin I, Kazanci N. Melatonin strongly interacts with zwitterionic model membranes-evidence from Fourier transform infrared spectroscopy and differential scanning calorimetry. Biochim Biophys Acta - Biomembr. 2005;1668:215–22.
23. Korkmaz F, Severcan F. Effect of progesterone on DPPC membrane: evidence for lateral phase separation and inverse action in lipid dynamics. Arch Biochem Biophys. 2005;440:141–7.
24. Potamitis C, Chatzigeorgiou P, Siapi E, Viras K, Mavromoustakos T, Hodzic A, Pabst G, Cacho-Nerin F, Laggner P, Rappolt M. Interactions of the AT_1 antagonist valsartan with dipalmitoylphosphatidylcholine bilayers. Biochim Biophys Acta. 2011;1808:1753–63.
25. Ergun S, Demir P, Uzbay T, Severcan F. Agomelatine strongly interacts with zwitterionic DPPC and charged DPPG membranes. Biochim Biophys Acta. 2014;1838:2798–806.
26. Riske KA, Barroso RP, Vequi-Suplicy CC, Germano R, Henriques VB, Lamy MT. Lipid bilayer pre-transition as the beginning of the melting process. Biochim Biophys Acta. 2009;1788:954–63.
27. Londoño-Londoño J, Lima VRD, Jaramillo C, Creczynski-pasa T. Hesperidin and hesperetin membrane interaction: understanding the role of 7-*O*-glycoside moiety in flavonoids. Arch Biochem Biophys. 2010;499:6–16.
28. Bilge D, Kazanci N, Severcan F. Acyl chain length and charge effect on Tamoxifen–lipid model membrane interactions. J Mol Struct. 2013;1040:75–82.
29. Fox CB, Harris JM. Confocal Raman microscopy for simultaneous monitoring of partitioning and disordering of tricyclic antidepressants in phospholipid vesicle membranes. J Raman Spectrosc. 2010;41:498–507.
30. Pickholz M, Oliveira ON, Skaf MS. Interactions of chlorpromazine with phospholipid monolayers: effects of the ionization state of the drug. Biophys Chem. 2007;125:425–34.
31. Gidalevitz D, Ishitsuka Y, Muresan AS, Konovalov O, Waring AJ, Lehrer RI, Lee KYC. Interaction of antimicrobial peptide protegrin with biomembranes. P Natl Acad Sci USA. 2003;100:6302–7.

32. Chen X, Huang Z, Hua W, Castada H, Allen HC. Reorganization and caging of DPPC, DPPE, DPPG, and DPPS monolayers caused by dimethylsulfoxide observed using brewster angle microscopy. Langmuir. 2010;26:18902–8.
33. Brouillard R, Iacobucci GA, Sweeny JG. Chemistry of anthocyanin pigments. 9. UV–Visible spectrophotometric determination of the acidity constants of apigeninidin and three related 3-deoxyflavylium salts. J Am Chem Soc. 1982;104:7585–90.
34. Drabent R, Pliszka B, Huszcza-Ciołkowska G, Smyk B. Ultraviolet fluorescence of cyanidin and malvidin glycosides in aqueous environment. Spectrosc Lett. 2007;40:165–82.
35. Figueiredo P, Lima JC, Santos H, Wigand M-C, Brouillard R, Maqanita AL, Pina F. Photochromism of the synthetic 4′,7-dihydroxyflavylium chloride. J Am Chem Soc. 1994;116:1249–54.
36. Lasic DD. Liposomes: from physics to applications. 1st ed. Amsterdam: Elsevier Science Ltd; 1993.
37. Poklar Ulrih N, Maričić M, Ota A, Šentjurc M, Abram V. Kaempferol and quercetin interactions with model lipid membranes. Food Res Int. 2015;71:146–54.
38. Lakowicz JR. Principles of fluorescence spectroscopy. New York: Springer; 2006.
39. Watts A, Harlos K, Maschke W, Marsh D. Control of the structure and fluidity of phosphatidylglycerol bilayers by pH titration. Biochim Biophys Acta. 1978;510:63–74.
40. Wesołowska O, Gasiorowska J, Petrus J, Czarnik-Matusewicz B, Michalak K. Interaction of prenylated chalcones and flavanones from common hop with phosphatidylcholine model membranes. Biochim Biophys Acta. 2014;1838:173–84.
41. Pruchnik H, Bonarska-Kujawa D, Kleszczyńska H. Effect of chlorogenic acid on the phase transition in phospholipid and phospholipid/cholesterol membranes. J Therm Anal Calorim. 2014;118:943–50.
42. Cater BR, Chapman D, Hawes SM, Saville J. Lipid phase transitions and drug interactions. Biochim Biophys Acta. 1974;363:54–69.
43. Papahadjopoulos D, Jacobson K, Poste G, Shepherd G. Effects of local anesthetics on membrane properties. I. Changes in the fluidity of phospholipid bilayers. Biochim Biophys Acta. 1975;394:504–19.
44. Brouillard R. Chemical structure of anthocyanins. In: Markakis P, editor. Anthocyanins as food color. New York: Academic Press; 1982. p. 1–40.
45. Saija A, Bonina F, Trombetta D, Tomaino A, Montenegro L, Smeriglio P, Castelli F. Flavonoid-biomembrane interactions: a calorimetric study on dipalmitoylphosphatidylcholine vesicles. Int J Pharm. 1995;124:1–8.
46. Ionov M, Klajnert B, Gardikis K, Hatziantoniou S, Palecz B, Salakhutdinov B, Cladera J, Zamaraeva M, Demetzos C, Bryszewska M. Effect of amyloid beta peptides Aβ_{1-28} and Aβ_{25-40} on model lipid membranes. J Therm Anal Calorim. 2010;99:741–7.
47. Bonarska-Kujawa D, Pruchnik H, Oszmiański J, Sarapuk J, Kleszczyńska H. Changes caused by fruit extracts in the lipid phase of biological and model membranes. Food Biophys. 2011;6:58–67.
48. Xu X, London E. The effect of sterol structure on membrane lipid domains reveals how cholesterol can induce lipid domain formation. Biochem US. 2000;39:843–9.
49. PubChem [Internet]. [cited 2014 Aug 25]. https://pubchem.ncbi.nlm.nih.gov/search/#collection=compounds.
50. Smith EA, Dea PK. Differential scanning calorimetry studies of phospholipid membranes: the interdigitated gel phase. In: Elkordy AA, editor. Applications of calorimetry in a wide context—Differential scanning calorimetry, isothermal titration calorimetry and microcalorimetry. InTech; 2013. p. 407–44.
51. Hribar U, Poklar Ulrih N. The metabolism of anthocyanins. Curr Drug Metab. 2014;15:3–13.
52. Ota A, Abramovič H, Abram V, Poklar Ulrih N. Interactions of *p*-coumaric, caffeic and ferulic acids and their styrenes with model lipid membranes. Food Chem. 2011;125:1256–61.
53. Abram V, Berlec B, Ota A, Šentjurc M, Blatnik P, Poklar Ulrih N. Effect of flavonoid structure on the fluidity of model lipid membranes. Food Chem. 2013;139:804–13.
54. Poklar Ulrih N, Ota A, Šentjurc M, Kure S, Abram V. Flavonoids and cell membrane fluidity. Food Chem. 2010;121:78–84.